Applied Soft Computing 70 (2018) 318–329

Contents lists available at ScienceDirect

Applied Soft Computing

journal homepage: www.elsevier.com/locate/asoc

Robust predictive control of wheel slip in antilock braking systems based on radial basis function neural network

Hossein Mirzaeinejad

Department of Mechanical Engineering, Shahid Bahonar University of Kerman, Jomhoori Eslami Blvd, Kerman, Iran

ARTICLE INFO

Article history:
Received 14 October 2017
Received in revised form 4 May 2018
Accepted 26 May 2018
Available online 29 May 2018

Keywords:
Anti-lock brake system
Nonlinear predictive control
RBF neural network
Robustness
Wheel slip

ABSTRACT

Anti-Lock Braking System (ABS) is a well-known technology for vehicle safety enhancement during hard braking. The wheel slip control has been a challenging problem due to a complex behavior of the tire and strong nonlinearity in a braking process. Furthermore, the system is subjected to unknown uncertainties that would arise from changing the vehicle parameters and un-model dynamics. Thus, it is required to design a nonlinear robust control law for ABS to overcome these problems. In this paper, a novel robust prediction-based controller for ABS is proposed that guarantees the stability against uncertainties. An optimal control law is firstly designed for ABS using nonlinear predictive method. Then, the unknown uncertainties are adaptively approximated utilizing a radial basis function neural network (RBFNN). The Lyapunov approach is employed to develop an update control law to determine the network weights. Finally, some simulations are conducted to examine the performance of the proposed control system for tracking the reference wheel slip in the presence of uncertainties in different maneuvers. Also, the performance of the proposed controller is compared with the conventional sliding mode controller (SMC) through simulation results.

1. Introduction

Many active safety devices have been developed to assist the driver to improve the vehicle safety during dangerous conditions. Among them, Anti-Lock Braking System (ABS) is a common well-known active safety technology to control of automotive braking systems. In a hard braking situation, the wheels might lock and the braking forces fall to their sliding values and the lateral forces are reduced to almost zero [1]. In this manner, the stopping distance will be increased and the directional stability of vehicle in turning maneuvers will be lost. Hence, the longitudinal wheel slip has significant role in affecting the performance of braking, traction and stability control systems in ground vehicles. The ABS is known as a good solution to maintain the wheel slip at desired value and prevent the wheel from locking. As a result, the shortened stopping distance is obtained and the safety and the vehicle steerability are enhanced. In another application, the ABS is used in electronic stability control (ESC) systems to provide the required yaw moment for stabilizing vehicle lateral dynamics by differential braking strategy [2].

Due to a complex behavior of the tire-road interaction, nonlinear dynamics of a braking process [3] and model uncertainties, the control of wheel slip has been a challenging problem [4]. The high degree of nonlinearity is as a result of tire force saturation behavior. Also, the main sources of uncertainties existing in vehicle dynamics can be considered as a result of changing the vehicle parameters and tire-road friction coefficient, and un-modelled dynamics. These uncertainties may significantly degrade the control performance, and thus robustness achievement is the key issue while designing the ABS controller.

It is found from the above discussion that a nonlinear robust control law should be designed for the ABS to solve these problems. In this respect, various controllers have been presented, which use the techniques of gain scheduling control [5], Backstepping approach [6], extremum seeking algorithm [7], fuzzy method [8], and so on. Sliding mode control (SMC) methods have been frequently used because of their potential to cope with nonlinearities and intrinsic robustness [9–13]. An intelligent exponential sliding-mode control system has been designed for wheel slip control in ABS [14]. In this work, a functional recurrent fuzzy neural network uncertainty estimator is proposed to approximate the unknown nonlinear term of ABS dynamics. In [15], a fractional order sliding model controller (FOSMC) is combined with Fuzzy logical control (FLC) to enhance the performance of FOSMC for ABS in compared with

E-mail address: h_mirzaeinejad@uk.ac.ir

https://doi.org/10.1016/j.asoc.2018.05.043
1568-4946/

conventional SMC. A self-tuning PID controller with integration of fuzzy and genetic algorithms (GAs) has been designed for ABS which minimizes the stopping distance [16]. Fuzzy logic has been integrated with the neural model to control the braking pressure to achieve maximum braking force [4]. Dincmen et al. [7] employed extremum seeking algorithm to design wheel slip controller which improves the lateral stability of the vehicle during emergency braking. Qiu et al. [6] developed backstepping dynamic surface control in conjunction with an asymmetric barrier Lyapunov function to maintain wheel slip within stable region for an electric aircraft landing system. Intelligent control can be able to cope with uncertainties which cannot be measured and may be changed during different conditions [17]. Soft computing techniques are extensively utilized for modelling and control in various industrial areas [18,19]. In [20], a contrast-based Fruit Fly Optimisation Algorithm (c-FOA) is applied to the suspension design problem. A combination of fuzzy logic and nature-inspired optimization including of a Simulated Annealing (SA) algorithm and a Particle Swarm Optimization (PSO) algorithm is proposed for modeling aspect in ABS [21]. Radial basis function neural networks (RBFNNs) are one of the more popular neural networks. Compared with the standard feedforward back propagation networks, RBFNNs have the advantages of faster learning speed and less chance falling into local minimal convergence [11,12]. It has been frequently applied mainly due to its computational efficiency in many fields, such as identification, control and pattern recognition [22–26]. Like neural networks and fuzzy inference systems, RBFNNs were also proven to be universal approximator [27]. The fast training of networks due to the simple structure of RBFNNs makes it easier to be designed and implemented. Also, RBFNNs have strong tolerance to input noise, which enhances the stability of the designed systems [28]. One challenge for the RBFNN modelling method is how to determine the RBF-NN parameters reasonably. In [29], the cuckoo search algorithm with membrane communication mechanism is proposed to optimize RBFNNs parameters. Robnik-Sikonja [30] presented a radial basis function network based generator of semi artificial data with similar properties to the original data, which enables the development and testing of different data mining algorithms and the optimization of their parameters. Tian et al. [31] proposed a novel algorithm for the construction of radial basis function neural network classifier based on subspace learning. In [32], a new cooperative learning method for RBFNNs based on PSO was applied for solving function approximation and classification problems with improved accuracy. In another work, GAs were used in conjunction with particle swarms to optimize a neural network for predicting rainfall [33].

In our previous studies, the wheel slip controllers of ABS with different versions include of cheap and expensive control strategies using a predictive method have been presented [34–36]. Also, the emergency braking on a split-μ road is considered [37,38] in which an optimal nonlinear algorithm for proper distribution of the tire braking forces is proposed. The main idea in these works is that the nonlinear response of a continuous nonlinear vehicle dynamics model is predicted. Then, a pointwise minimization performance index that penalizes the difference between the predicted and desired responses of the wheel slip is utilized to find the current control input. To increase the controller robustness, the integral feedback method is applied to the design method [34]. However, the integral feedback technique causes to increase the control system order which complicates controller implementation. As a continuation of this work, in the present paper, the RBFNN will be developed to approximate the unknown uncertainties. By doing this, the controller robustness can be increased without increasing the order of the control system and thus providing easier implementation of the controller. Additionally, the regulation of the free control parameters is not needed when the maneuver is changed because of updating the proposed control law. These are the main differences between the present work and previous ones.

Application of classic optimal control theory to the non-linear system requires that the derived nonlinear two-point boundary value (TPBV) problem or Hamilton–Jacobi–Bellman (HJB) partial differential equations are solved [39]. These methods suffer from computational load because of online optimization process. It is very difficult or even impossible to find an analytical solution for this problem. Also, numerical computation approaches are not easy to implement and need online dynamic optimization. In fact, the computational load imposes challenges for real applications. In this research, at first a controller is developed for ABS based on the nonlinear predictive approach by the response prediction of a continuous non-linear vehicle dynamics model. The proposed control law is given in an analytical form which is easy to solve and implement. Moreover, because of existence of unknown uncertainties that would arise from changing the vehicle parameters and unmodel dynamics, the RBFNN is appended to the design method to increase the robustness of the controller. The Lyapunov approach is employed to develop an update control law to determine the network weights. Finally, some simulations are conducted to examine the effectiveness of the proposed control system for tracking the reference wheel slip in the presence of uncertainties in different maneuvers. The performance of the proposed control scheme is compared with the sliding mode controller (SMC) through simulation results. The performed analysis along with the simulation results demonstrates that the controller with RBFNN can handle nonlinearity and uncertainty of the model successfully.

The rest of this paper is organized as follows. The longitudinal dynamic model of a vehicle during a braking maneuver and a reference model for wheel slip are presented in Section 2, followed by the control system design in Section 3. In Section 4, simulation results are given. Finally, the conclusion is provided in Section 5.

2. Mathematical modeling

2.1. Vehicle model

Here, a nonlinear quarter vehicle model which has essential characteristics of the actual model is considered as design model to control the wheel slip. This model has frequently utilized to develop the longitudinal wheel slip controller [34,40].

The governing equations for the nonlinear quarter vehicle model of Fig. 1 are as follows:

$$\dot{v}_x = \frac{-F_x}{M} \tag{1}$$

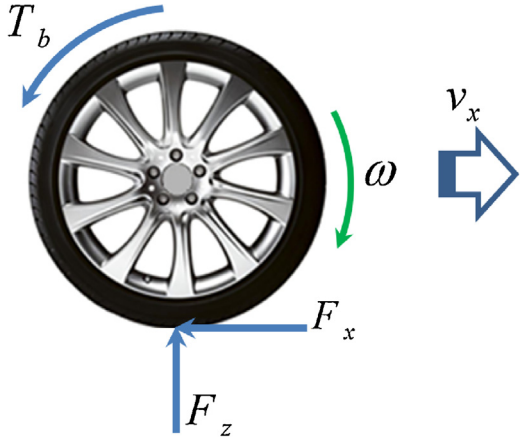

Fig. 1. Wheel free body diagram.

$$\dot{\omega} = \frac{1}{I_w}(RF_x - T_b) \tag{2}$$

where v_x is the longitudinal velocity of the vehicle, F_x is the longitudinal braking force, M is the mass of the quarter vehicle, ω is the wheel angular velocity, I_w is the moment of inertia of the wheel, R is the radius of the wheel and T_b is the braking torque. The nonlinear Dugoff tire model which considers the saturation property of tire force is used to model the longitudinal braking force [41].

Taking the time derivative of the wheel slip during braking, $\lambda = 1 - R\omega/v_x$, and substituting Eqs. (1) and (2) into the derivative form yields:

$$\dot{\lambda} = -\frac{1}{v_x}\left(\frac{F_x}{M}(1-\lambda) + \frac{R^2}{I_w}F_x\right) + \left(\frac{R}{I_w v_x}\right)T_b \tag{3}$$

Eq. (1) can be written as:

$$\dot{\lambda} = f(\boldsymbol{X}) + g(\boldsymbol{X})T_b \tag{4}$$

where $\boldsymbol{X} = [x_1\ x_2]^T = [v_x\ \lambda]^T$ is the state vector and T_b represents the control input. From Eqs. (3) and (4), nonlinear functions $f(\boldsymbol{X})$ and $g(\boldsymbol{X})$ can be written accordingly as:

$$\begin{aligned} f(\boldsymbol{X}) &= \frac{1}{v_x}\left(\frac{F_x}{M}(1-\lambda) + \frac{R^2}{I_w}F_x\right) \\ g(\boldsymbol{X}) &= \frac{R}{I_w v_x} \end{aligned} \tag{5}$$

Assuming that all the system parameters are well known, the nominal model of system described by Eq. (4) can be represented as following:

$$\dot{\lambda} = f_n(\boldsymbol{X}) + g_n(\boldsymbol{X})T_b \tag{6}$$

where f_n and g_n are the nominal values of f and g, respectively.

Deviation of f and g from their nominal values (f_n and g_n) can be a result of uncertainties in the vehicle model and road condition. If there exist system uncertainties due to no full knowledge of the system model such as parameter variations, un-model dynamics and disturbances, the non-linear system described by Eq. (4) can be modified as:

$$\dot{\lambda} = [f_n(\boldsymbol{X}) + \Delta f(\boldsymbol{X})] + [g_n(\boldsymbol{X}) + \Delta g(\boldsymbol{X})]T_b \quad = f_n(\boldsymbol{X}) + g_n(\boldsymbol{X})T_b + L \tag{7}$$

where $\Delta f(\boldsymbol{X})$ and $\Delta g(\boldsymbol{X})$ represent the unknown uncertainties; L as a single term is called lumped uncertainty and defined as $L = \Delta f(\boldsymbol{X}) + \Delta g(\boldsymbol{X})T_b$ with the assumption $L \le N_1$, in which N_1 is a positive constant.

The following reference model [34] is considered to be tracked by the wheel slip controller:

$$\lambda_d(t) = \lambda_{opt} - \lambda_{opt}e^{-20t} \tag{8}$$

where $\lambda_{opt} = 0.15$ is the optimum wheel slip.

3. Control system design

3.1. Prediction-based controller (PbC)

In this section, a prediction-based controller for ABS will be designed. Here, it is assumed that all the states are available for feedback control. The control objective is to find a suitable control law so that the wheel slip can track it's reference model λ_d despite the presence of unknown uncertainties. Defining the tracking error as following:

$$e(t) = \lambda(t) - \lambda_d(t) \tag{9}$$

where $\lambda(t)$ is the system output.

In order to develop the wheel slip control law, the prediction-based control method is applied. A point-wise performance index minimizing the next instant tracking error is defined as follows

$$J[T_b(t)] = \frac{1}{2}e^2(t+h) \tag{10}$$

where, h is the predictive horizon. It should be noted that the cheap control strategy [34] is employed here in which the control input T_b is not penalized. However, how to achieve a minimum control effort will be discussed at the rest of design process.

Regarding the prediction-based control method, the nonlinear response of the longitudinal slip of the wheel is first predicted by Taylor series expansion and then the performance index can be obtained as a function of control input T_b. In this respect, to develop the predicted response in terms of current control input, $\lambda(t+h)$ is expanded by a qth-order Taylor series at t

$$\lambda(t+h) = \lambda(t) + h\dot{\lambda}(t) + \frac{h^2}{2!}\ddot{\lambda}(t) + \cdots + \frac{h^q}{q!}\lambda^{(q)}(t) \tag{11}$$

The expansion order q is determined by the control order plus the relative degree of the nonlinear system [42]. According to the system model, the output has the well-defined relative degree, $\rho = 1$, which is determined as the lowest order of the derivative of the output in which the input first appears explicitly [43]. It is proved to achieve a minimum control effort, the control order in controller design process should be selected as low as possible [42]. In this paper, the control order is limited to be zero so that the control effort will be a constant in the prediction interval

$$\frac{d}{d\tau}T_b(t+\tau) = 0 \ \ for\ \tau \in [0,\ h] \tag{12}$$

This selection, i.e. zero control order, makes the derivatives of control input disappear in the prediction of each output and obtains relatively adequate performance for non-linear systems with lower relative degrees [42]. Generally, the control order is considered as a design parameter which makes a compromise between performance and input energy requirements.

From discussion above, it is concluded that the first-order Taylor series is sufficient to expand the wheel slip and its desired value as follows

$$\lambda(t+h) = \lambda(t) + h(f_n(\boldsymbol{X}) + g_n(\boldsymbol{X})T_b + L) \tag{13}$$

$$\lambda_d(t+h) = \lambda_d(t) + h\dot{\lambda}_d(t) \tag{14}$$

Substituting the Eqs. (13) and (14) into Eq. (10), the performance index is obtained as a function of control input T_b

$$J(T_b) = \frac{1}{2}\left[e + h(f_n(\boldsymbol{X}) + g_n(\boldsymbol{X})T_b + L)\right]^2 \tag{15}$$

Finally, applying the optimality condition as

$$\frac{\partial J}{\partial T_b} = 0 \tag{16}$$

Leads to the following control law

$$T_b = -\frac{1}{hg_n(\boldsymbol{X})}\left[e + h\left(f_n(\boldsymbol{X}) + L - \dot{\lambda}_d\right)\right] \tag{17}$$

Theorem 1 ([44]). Let J be the quadratic function defined by

$$J(u) = g^T u + \frac{1}{2}u^T B u \tag{18}$$

then, J has a unique minimizer if and only if B is positive definite matrix.

The performance index (15) has a quadratic form and it can be easily shown that B is a positive scalar. Therefore, according to the Theorem 1, the necessary condition of (16) will be also sufficient for global optimality at each instant.

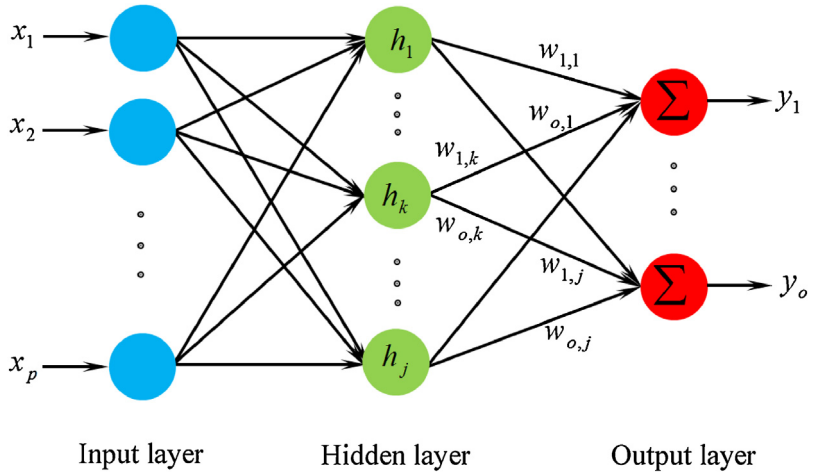

Fig. 2. Schematics of the RBFNN with multiple outputs.

Assuming that the system dynamics are well known which means that L is known, the presented control law described by Eq. (17) can guarantee the stability in the Lyapunov sense. Choosing the Lyapunov function as

$$V_1 = \frac{1}{2}e^2 \tag{19}$$

and differentiating Eq. (19) with respect to time and using Eqs. (7) and (17) leads to

$$\begin{aligned} \dot{V}_1 = e\dot{e} \quad &= e\left(\dot{\lambda} - \dot{\lambda}_d\right) \\ &= e\left(f_n(\boldsymbol{X}) + g_n(\boldsymbol{X})T_b + L - \dot{\lambda}_d\right) \\ &= e\left(-\frac{1}{h}e\right) = -\frac{1}{h}e^2 \le 0 \end{aligned} \tag{20}$$

Therefore, the control law given by Eq. (17) asymptotically stabilizes the system of Eq. (7). However, since the lumped uncertainty L is commonly unknown, the control law given by Eq. (17) is unrealizable in a practical application.

Applying the control law (17), which is based on the nominal model, in the actual model (7) leads

$$\dot{\lambda} = -\frac{1}{h}e - \hat{L} + \dot{\lambda}_d + L \tag{21}$$

From (9) and (21), the wheel slip tracking error dynamics is obtained as follows

$$\dot{e} + \frac{1}{h}e = L - \hat{L} \tag{22}$$

where $\hat{L}$ is the estimated value of L. Deviation of L from $\hat{L}$ will always lead to some tracking errors. However, the estimation error on L is assumed to be bounded by a constant $N_2 > 0$ as

$$|L - \hat{L}| < N_2 \tag{23}$$

Now, applying the bounds of Eq. (23) to the error dynamics (22) and solving the first order differential equation with zero initial condition, implies that the tracking error $e(t)$ is bounded within

$$|e(t)| < e_m \text{ for all } t \ge 0 \tag{24}$$

where

$$e_m = hN_2 \tag{25}$$

Eq. (25) indicates that the uncertainty estimation error will always lead to some tracking errors. However, the wheel slip error can be decreased by increasing the accuracy of estimation of lumped uncertainty L and the regulation of the free parameter h. Hence, for a certain estimation error, in order to reduce the tracking error further, one can decrease the value of h to some extent; otherwise the control energy will be large and oscillatory, because $1/h$ is seen as the controller gain in Eq. (17). This case will be further investigated in simulation studies. In the next section, the RBFNN will be developed to approximate the unknown lumped uncertainty L.

3.2. Radial basis function neural network (RBFNN)

It is proved that any continuous function over a compact set can be approximate by RBFNNs [27]. The RBFNN can be regarded as a feed-forward network composed of three layers of neurons [45]. The first layer is called the input layer, and it is consisted of source nodes for the input data. The second layer, which is the single hidden layer in the network, is made up of the radial basis functions. The nonlinear transformation is applied by these functions from the input layer into the hidden layer. The third layer is called the output layer, and it is constructed by the linear combination of the function responses. The structure of a standard RBFNN with multiple outputs is illustrated in Fig. 2.

In the input layer, $\boldsymbol{x} = \left[x_1\, x_2 \ldots x_p\right]^T$ is the input vector of the RBFNN. The Gaussian function is considered as the radial basis function in the hidden layer, which is described as follows

$$h_j(x) = exp\left(-\frac{\left|\left|x - c_j\right|\right|^2}{{\sigma_j}^2}\right) \quad j = 1, 2, \ldots, m \tag{26}$$

where $\|\cdot\|$ is the Euclidean norm, j is the jth neuron of the hidden layer and m denotes the number of the hidden neurons. Also, c_j and σ_j are the centers and width of the Gaussian function, respectively.

In the output layer, the RBFNN output will then be built up as the weighted linear combination of the outputs of the hidden neurons as following:

$$y_i = \sum_{j=1}^{m} w_{i,j}h_j(x), \quad i = 1, 2, \ldots, o \text{ and } \quad j = 1, 2, \ldots, m \quad = \boldsymbol{w_i}^T\boldsymbol{h}(\boldsymbol{x}) \tag{27}$$

where $\boldsymbol{h} = [h_1, \ldots, h_m]^T$ is the hidden output vector and $\boldsymbol{w_i} = \left[w_{i,1}, \ldots, w_{i,j}\right]^T$ stands for the weights vector of the network and $w_{i,j}$ is the connective weight between the jth hidden neuron and the oth neuron of the output layer.

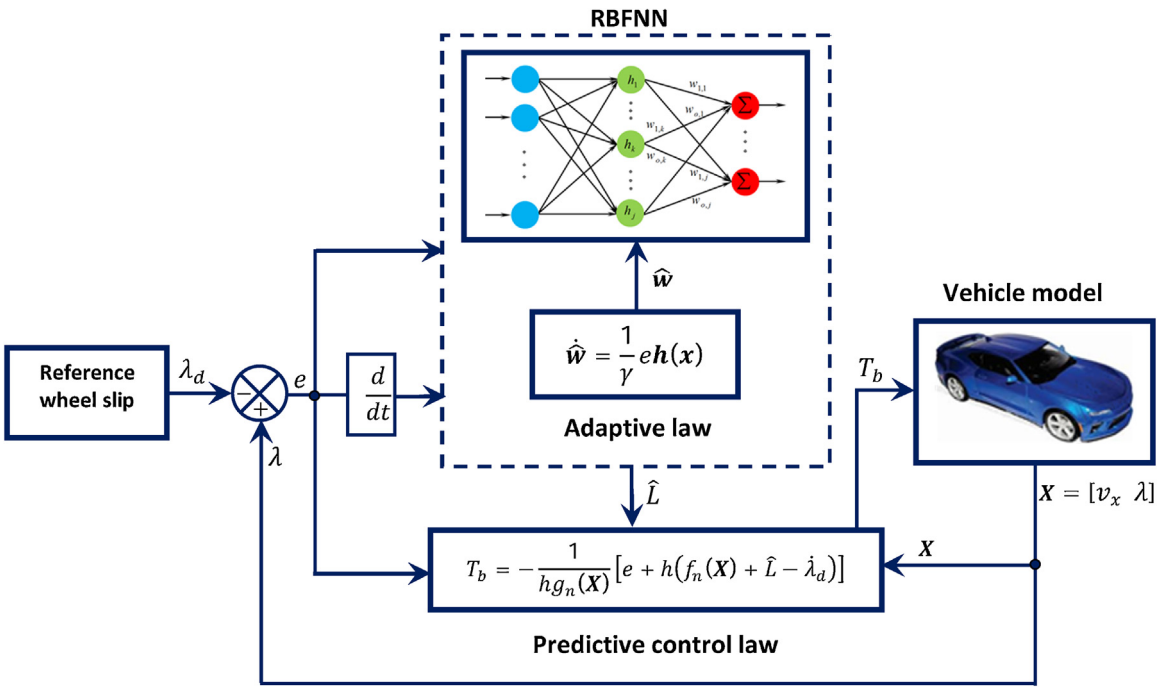

Fig. 3. Overall structure of the proposed control system.

Theorem 2 ([46]). For any given positive constant $\varepsilon > 0$ and for a continuous function $f(x)$ on a compact set Ω, there exists the RBFNN in the form of (27) such that:

$$sup_{x\varepsilon\Omega}|f(x) - \boldsymbol{w_i}^T\boldsymbol{h}| < \varepsilon \tag{28}$$

The above theorem indicates that the RBFNN is a universal approximator. This means that any continuous function on a compact set can be approximated by the RBFNN.

3.3. Radial basis function neural network prediction-based controller (RBFNN-PbC)

In designing a prediction-based controller for ABS, it is necessary to know the system dynamics. However, the accurate models are always difficult to formulate and the deviation of the system parameters from the nominal model are inevitable. To solve this problem, a prediction-based control system with RBFNN shown in Fig. 3 is proposed to control the wheel slip.

Here, the RBFNNs are adaptively employed to approximate the lumped uncertainty L. According to the universal approximation theorem, there exists a RBFNN to approximate the unknown lumped uncertainty L such that

$$L = \boldsymbol{w}^T\boldsymbol{h}(\boldsymbol{x}) + \varepsilon \tag{29}$$

where ε is the approximation error with the assumption $|\varepsilon| \le \varepsilon_N$, in which ε_N is a positive constant. The tracking error and its first derivative, $\boldsymbol{x} = [e, \dot{e}]$, are considered as the inputs of the RBFNN. Also, the output of RBFNN is as follows

$$\hat{L} = \hat{\boldsymbol{w}}^T\boldsymbol{h}(\boldsymbol{x}) \tag{30}$$

where $\hat{L}$ is the approximated value of L.

In the following, the Lyapunov synthesis approach is used to develop an adaptive control law to adjust the network weights. In the presence of modeling uncertainty the control law given by Eq. (17) can be rewritten with approximated value of L as follows

$$T_b = -\frac{1}{hg_n(\boldsymbol{X})}\left[e + h\left(f_n(\boldsymbol{X}) + \hat{L} - \dot{\lambda}_d\right)\right] \tag{31}$$

Substituting Eqs. (29) and (30) to wheel slip tracking error dynamics (22), yields

$$\dot{e} + \frac{1}{h}e = \tilde{\boldsymbol{w}}^T\boldsymbol{h}(\boldsymbol{x}) + \varepsilon \tag{32}$$

where $\tilde{\boldsymbol{w}} = \boldsymbol{w}^T - \hat{\boldsymbol{w}}^T$.

Defining the Lyapunov function as following

$$V_2 = \frac{1}{2}e^2 + \frac{1}{2}\gamma\tilde{\boldsymbol{w}}^T\tilde{\boldsymbol{w}} \tag{33}$$

where γ is a positive constant.

Then, differentiating Eq. (33) with respect to time and using Eq. (32) leads to

$$\begin{aligned}\dot{V}_2 &= e\dot{e} + \gamma\tilde{\boldsymbol{w}}^T\dot{\tilde{\boldsymbol{w}}} \\ &= e\left(-\frac{1}{h}e + \tilde{\boldsymbol{w}}^T\boldsymbol{h}(\boldsymbol{x}) + \varepsilon\right) - \gamma\tilde{\boldsymbol{w}}^T\dot{\hat{\boldsymbol{w}}} \\ &= \tilde{\boldsymbol{w}}^T\left(e\boldsymbol{h}(\boldsymbol{x}) - \gamma\dot{\hat{\boldsymbol{w}}}\right) + e\left(\varepsilon - \frac{1}{h}e\right)\end{aligned} \tag{34}$$

By choosing the adaptive law as

$$\dot{\hat{\boldsymbol{w}}} = \frac{1}{\gamma}e\boldsymbol{h}(\boldsymbol{x}) \tag{35}$$

Then, it can be obtained that

$$\dot{V}_2 = e\varepsilon - \frac{1}{h}e^2 \tag{36}$$

Finally the following form can be derived as

$$\dot{V}_2 \le |e|\left(-\frac{1}{h}|e| + \varepsilon_N\right) \tag{37}$$

So if $|e| \ge h\varepsilon_N$, then $\dot{V}_2 \le 0$ which means that the defined Lyapunov function will decrease gradually. Thus, it can be concluded from this analysis that the proposed controller is stable and the wheel slip tracking error will converge into a small error bound. When the accuracy of the RBFNN in approximation of lumped uncertainty L increases, the tracking error decreases. In the ideal

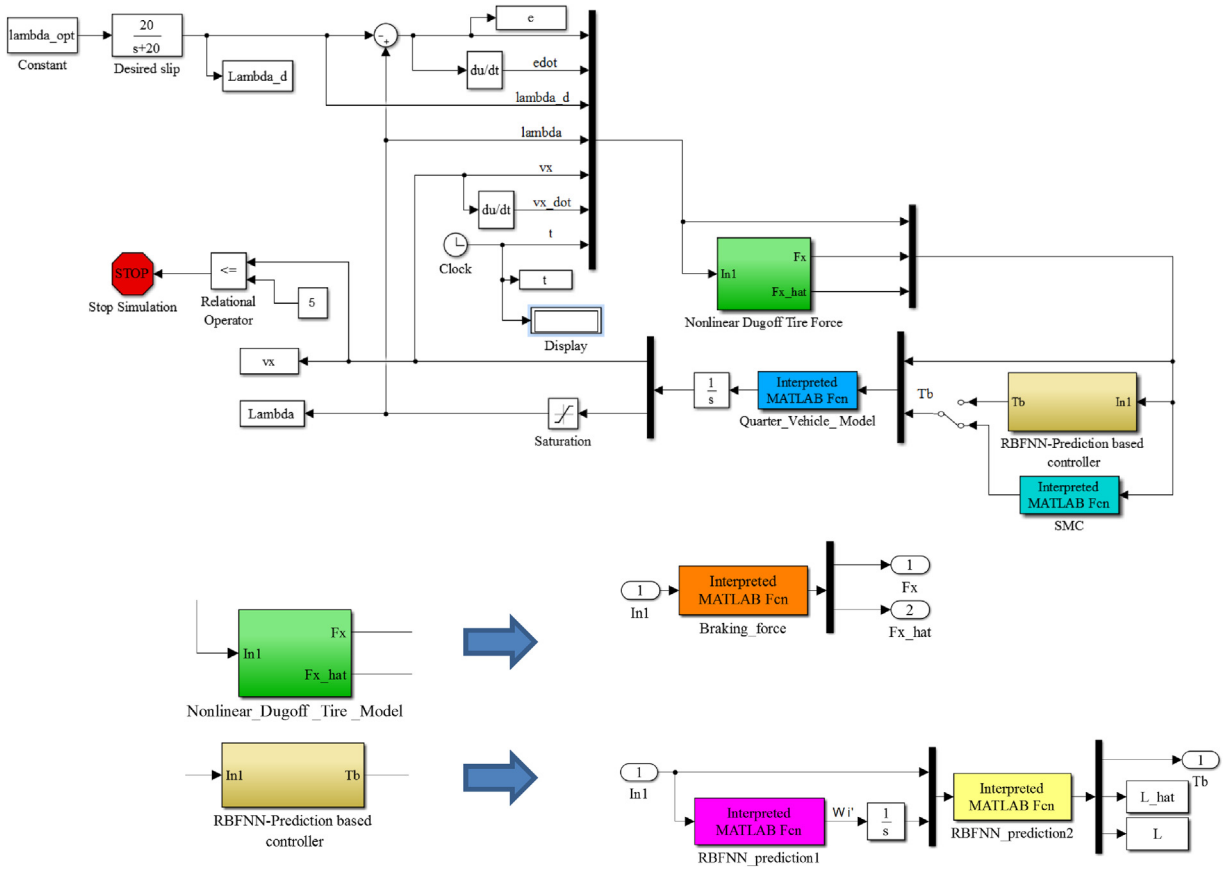

Fig. 4. The Simulink scheme of the proposed control system.

case, if the approximation error ε tends to zero then, the control law (31) asymptotically stabilizes the system.

4. Simulation results

In this section, simulation results are presented to evaluate the proposed controller performance. The values of the parameters of nominal model relevant to the case studied in simulation are $M = 455$ kg, $I_w = 1.7$ kgm^2, $R = 0.326$ m. The initial conditions of velocity and wheel slip are $v_x(0) = 20m/s$ and $\lambda(0) = 0$, respectively. Since, the wheel and vehicle velocity are nearly zero at the end of braking, the wheel slip tends to infinity. Thus, simulations are stopped when the vehicle is slowed to approximately 5 m/s.

In order to have a good performance of control system, the proposed controller parameters should be regulated properly. In this respect, note that the more the number of neurons in the hidden layer, the higher the control accuracy of the RBNNs, but too many hidden layer neurons will result in network complexity and excessive computing time. Therefore, the number of neurons in the hidden layer can be properly chosen by simulation experiments according to the requirements of practical control accuracy. Here, the number of neurons in the hidden layer is selected to be 5 to balance complexity and accuracy. The RBF centres, c_j, are selected by K-means method as one of the most well-known clustering methods. Also, the widths of the Gaussian functions,σ_j, are optimized using GA method. For all maneuvers, the prediction time is taken to be $h = 0.001$ s and $\gamma = 1e-5$. Also, the fixed step size in Simulink is selected to be 0.001 s. The structure of proposed control system is depicted in Fig. 3. Also, The Simulink scheme of the proposed control system is presented in Fig. 4. The Matlab programs used for simulation are given in Appendix A.

First, a comparison of the vehicle responses with and without control during braking on a dry road is shown in Fig. 5. The modeling uncertainty is not considered in this maneuver. The results show that the wheel of the vehicle without ABS has locked and thus the angular velocity of the wheel has become zero and a skid is occurred ($\lambda = 1$). In contrast, the reference wheel slip can be tracked very well in the controlled vehicle.

To investigate the effectiveness of the proposed controller, a comparison among the prediction-based controller (PbC) and the radial basis function neural network prediction-based controller (RBFNN-PbC) is made with regard to various maneuvers. Maneuver 1 is braking on a dry road ($\mu = 0.8$), maneuver 2 is braking on a slippery road ($\mu = 0.4$) and maneuver 3 is braking on a transition road in which a sudden change in the road conditions at $t = 1$ s is applied from slippery surface to dry surface.

The nominal system dynamics f_n and g_n are obtained based on nominal value reported at beginning of Section 4 assuming that the friction coefficients are known for dry and slippery roads. However, the nominal system dynamics are difficult to obtain in real ABS control. Hence, to examine the effect of modeling parametric uncertainties, some arbitrary uncertainties in the vehicle parameters are considered. Here, the parametric uncertainties include 30% in the vehicle mass, 30% in moments of inertia of the wheel I_w, −30% in longitudinal stiffness of the tire and 35% in tire-road friction coefficient.

Fig. 6 presents the comparison results of two controllers for maneuver 1. Fig. 6a indicates that the wheel slip error is significantly decreased with the RBFNN-PbC and is close to zero. Also, the control inputs are shown in Fig. 6b. For both controllers, the control inputs are smooth and free from oscillation. The lumped uncertainty L and its approximation $\hat{L}$ are compared in Fig. 6c. As

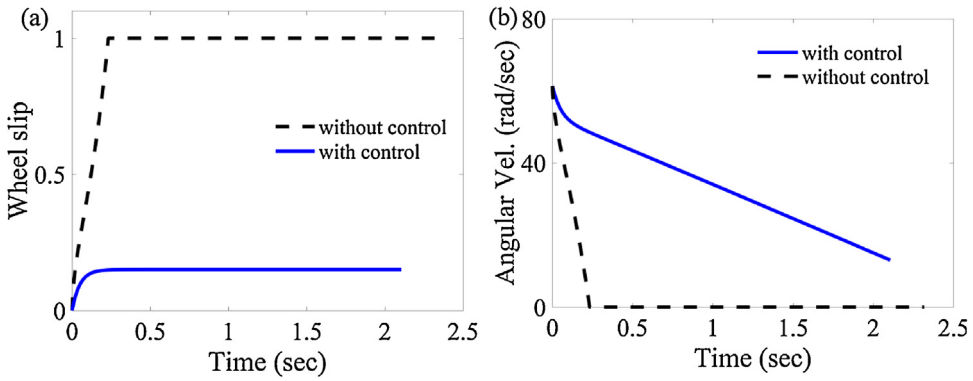

Fig. 5. Comparison of the responses of the controlled and uncontrolled vehicle during braking (a) wheel slip (b) wheel angular velocity.

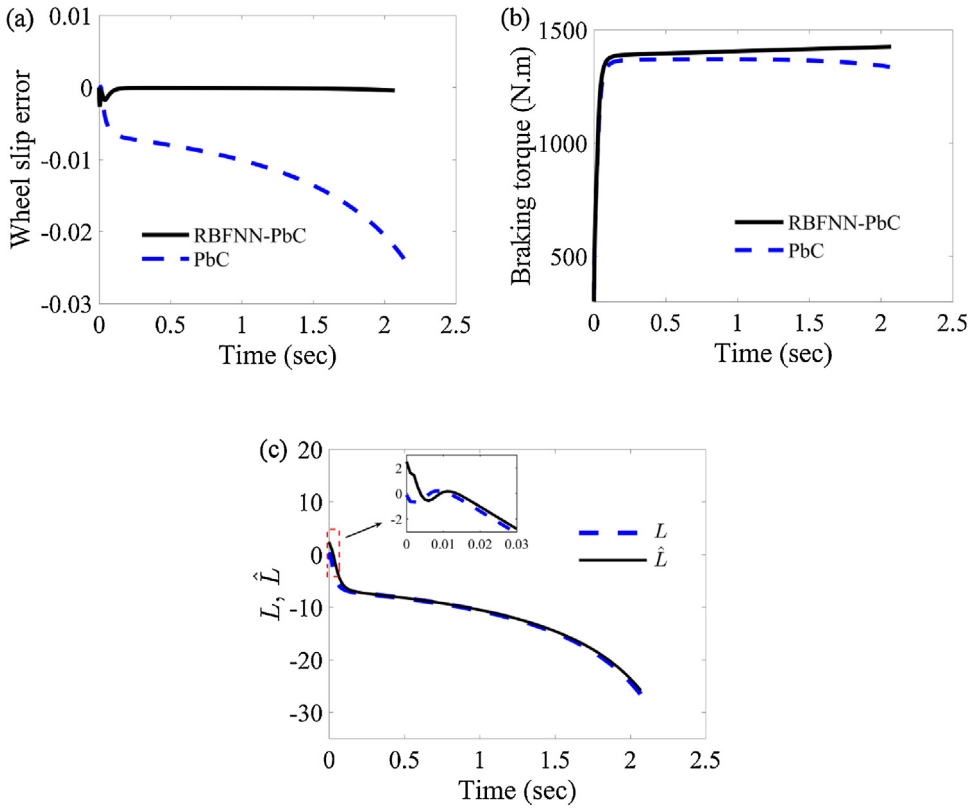

Fig. 6. Comparison of performances of the PbC and RBFNN-PbC for maneuver 1: (a) wheel slip tracking error, (b) braking torque and c) L and $\hat{L}$, maneuver 1.

it is seen, the RBFNN-PbC can accurately approximate the lumped uncertainty.

The prediction time h as a free design parameter can be regulated by considering the fact that, the slip tracking error can be reduced with decreasing prediction time h as stated by Eq. (25). However, the value of h can be decreased to some extent, otherwise, the control effort becomes large and oscillatory. This is due to the presence of $1/h$ as the controller gain in Eq. (17). This oscillation can be seen in Fig. 7 for smaller value of $h = 0.0006$. As stated before, the prediction time value for other simulation is considered as $h = 0.001$.

The simulation results for maneuver 2 are presented in Fig. 8. As can be seen, the same results as dry road are obtained in this maneuver too.

The maneuver 3 is considered to investigate the performance of controllers in a situation of road transition. In this maneuver, the road surface is changed from slippery to dry at 1 s. The simulation results for maneuver 3 are shown in Fig. 9. Also, in this maneuver, plots of the vehicle and wheel speed for two controllers are shown in Fig. 9c and d. The results indicate that the transient response for the road transition has been adapted well by the RBFNN-PbC with approximately zero error, while the wheel slip tracking error by PbC can be considerable. Additionally, for both cases the braking torque and speed are smooth without drastic oscillations at the transition time.

The tracking performance of the RBFNN-PbC is compared with the conventional sliding mode controller (SMC) [47,48]. It should be noted that the design parameters of the sliding mode controller are regulated in a way that the lowest tracking error is achieved. With any suitable changes in the regulation parameters, the error cannot be decreased any more and the responses begin to become oscillatory. The obtained results are illustrated in Fig. 10. As can be seen, the conventional sliding mode controller has higher tracking error in compared with the proposed controller. In addition, some chat-

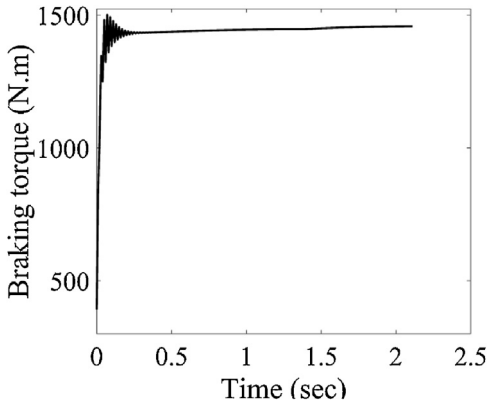

Fig. 7. Effect of a smaller value of prediction time ($h = 0.0006$) on the control energy.

Table 1
Comparison of performances of different controllers in various maneuvers.

Controller		PbC	RBFNN-PbC	SMC
Maneuver 1	$\int_0^{t_f} e^2 dt \times 10^8\,(sec)$	1495.5	1.42	1483.3
	$\int_0^{t_f} v_x dt\,(m)$	27.36	26.65	27.24
Maneuver 2	$\int_0^{t_f} e^2 dt \times 10^8\,(sec)$	294.2	1.25	269.2
	$\int_0^{t_f} v_x dt\,(m)$	50.01	49.38	49.95
Maneuver 3	$\int_0^{t_f} e^2 dt \times 10^8\,(sec)$	1405.3	8.6	1398.3
	$\int_0^{t_f} v_x dt\,(m)$	35.33	34.52	35.29

tering can be seen in the results obtained by conventional sliding mode controller at the beginning of the considered maneuver.

The dynamic performance of different controllers is compared in Table 1. The values of stopping distance and the integral value of squared tracking error for different controllers in various maneuvers are reported in this table. The wheel slip tracking error obtained by the RBFNN-PbC is remarkably reduced. In fact, the RBFNN-PbC reduces the effect of model uncertainties on the wheel slip tracking error during braking as mentioned in the Section 3.2.

The simulation results for all maneuvers show that the RBFNN-PbC can achieve favorable performance such as good parameter variation rejection and good tracking accuracy without oscillatory braking torque. The results are good, only some error is present at the initial learning phase, since the adaptive law in the RBFNN uncertainty estimator is initialized from zero.

5. Conclusion

The main difficulty arising in the design of ABS control law is due to the strong nonlinearity and unknown uncertainties. To overcome this problem, this paper proposes a controller, in which the predictive control method in conjunction with RBFNN is applied to achieve a good robustness and tracking performance. The proposed control law is given in an analytical form which is easy to solve and implement. The simulation results show that the proposed control system ensures the wheel slip tracking error obtained by the RBFNN-PbC is remarkably reduced. Finally, the simulation studies show the proposed controller proves to be better than a sliding controller designed in the prevalent papers for anti-lock braking systems. The major contributions of this paper are: 1) Designing a new robust prediction-based controller in conjunction with radial basis function neural network (RBFNN) for vehicle braking system. 2) The uncertainty estimator can online approximate the unknown term in the system dynamics of an ABS. 3) The Lyapunov function is proposed to determine the online parameters of the adaptation law. 4) Robustness analysis of the controller is performed with respect to the realistic uncertainties. 5) The robustness against road

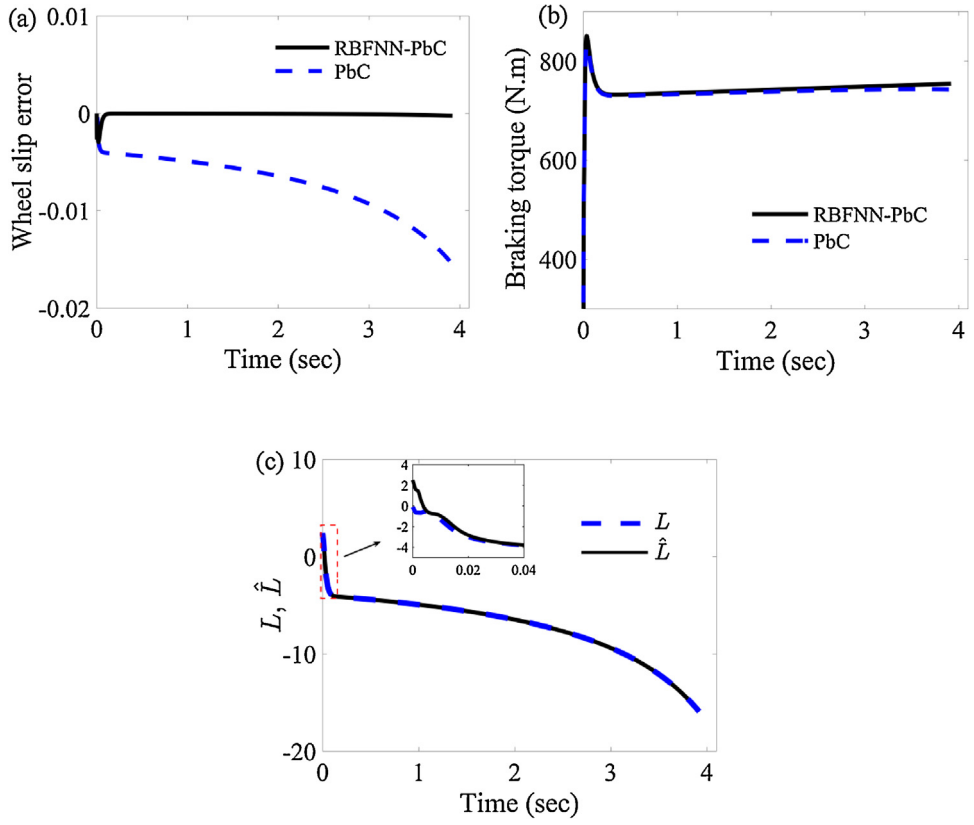

Fig. 8. Comparison of performances of the PbC and RBFNN-PbC for maneuver 2: (a) wheel slip tracking error (b), braking torque and (c) L and $\hat{L}$.

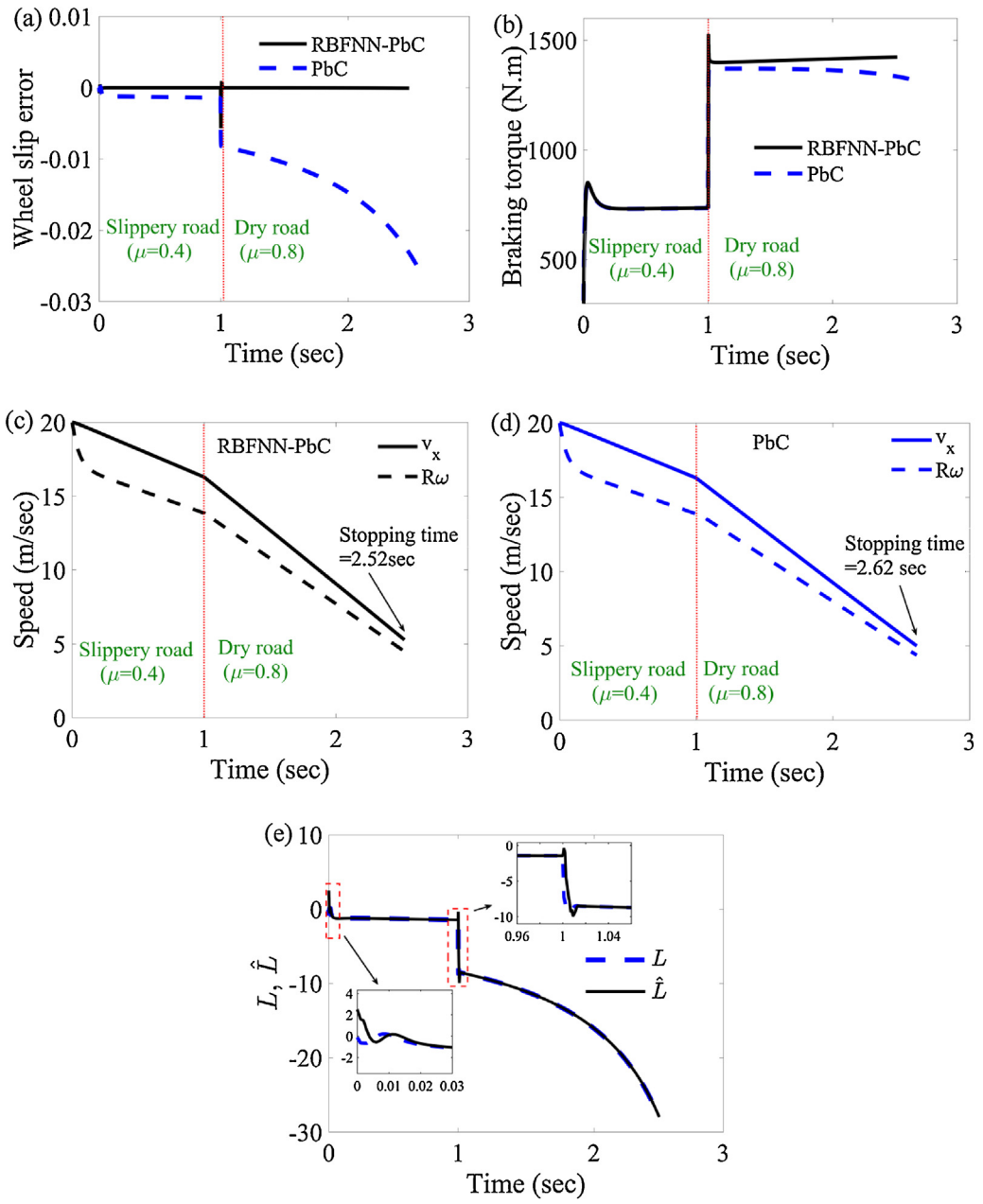

Fig. 9. Comparison of performances of the PbC and RBFNN-PbC for maneuver 3: (a) wheel slip tracking error, (b) braking torque, (c) and (d) wheel and vehicle speed and (e) L and $\hat{L}$.

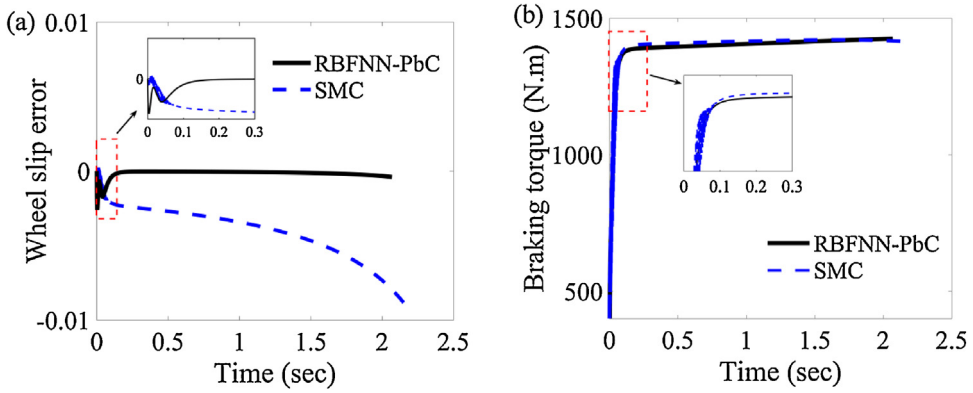

Fig. 10. Comparison of performances of the RBFNN-PbC and SMC for maneuver 1: (a) wheel slip tracking error and (b) braking torque.

conditions is examined, and simulation results are compared with previous works.

Appendix A.

Matlab programs

(a) main file:

```
clc
clear all
global R l hcg mw mvs mt_hat It_hat c1_hat epsr vx0 mu_hat g cc bb NL gamma
hh mt c1 It mu alfa lambda_opt
% system parameters
R=0.326;            % Wheel radius
l=2.5;              % Wheelbase
hcg=0.5;            % Center of gravity height
mw=40;              % Wheel mass
mvs=1660;           % vehicle sprung mass
mt_hat=445;         % Nominal value for the mass of the quarter vehicle=.25*mvs+mw;
It_hat=1.7;         % Nominal value for the moment of inertia of the wheel
c1_hat=50000;       % Nominal value for the longitudinal tire stiffness
epsr=.015;          % Parameter of the Dugoff model
g=9.81;             % Gravity acceleration
lambda_opt=0.15;    % Constant for the desired value of wheel slip
vx0=20;             % Initial value of the longitudinal velocity (m/s)
mu_hat=0.6;         % Nominal value for the friction coefficient
alfa=0;             % Lateral wheel slip of tire
%==================================================
% uncertainty
mu=0.8;                              % Actual value for the friction coefficient of dry road
c1= c1_hat+(-30*1*c1_hat)/100;       % Actual value for the longitudinal tire stiffness
mt=mt_hat+(30*1*mt_hat)/100;         % Actual value for the mass of the quarter vehicle
It= It_hat+(30*1*It_hat)/100;        % Actual value for the moment of inertia of the wheel
%==================================================
% Controllers Parameters
hh=0.001;                            % Prediction time
%==================================================
%RBFNN Parameters
gamma=.00001;                        % Positive constant
NL=5;                                % Number of neurons in the hidden layer
c = [-0.25  -0.09  0.002  0.01  0.23
     -1.54  -0.54  0.005  0.2   0.44]% Centers of the Gaussian functions
bb = [ 3.2  1.3   2.1   1.4   2.7];  % Widths of the Gaussian functions
%==================================================
% Run the simulation
sim('proposed_control_system')
%==================================================
```

(b) Nonlinear_ Dugoff _Tire _Force Subsystem

(b1)Braking force function

```
function y=Braking_force(x)
global l hcg mvs mt c1 epsr g mt_hat c1_hat mu_hat mu
lambda=x(4);
vx=x(5);
vxdot=x(6);
%============================================================
% Calculation of the tire normal load
Fz=mt*g-mvs*hcg*vxdot/(2*l);                % Actual normal load
Fz_hat=mt_hat*g-mvs*hcg*vxdot/(2*l);        % Nominal normal load
%============================================================
% Calculation of the braking force based on Dugoff model
s=mu*Fz*(1-epsr*vx*lambda)*(1-lambda)/(2*c1*lambda);
s_hat=mu_hat*Fz_hat*(1-epsr*vx*lambda)*(1-lambda)/(2*c1_hat*lambda);
if s<1
fs=s*(2-s);
else
    fs=1;
end
if s_hat<1
   fs_hat=s_hat*(2-s_hat);
```

```
else
   fs_hat=1;
end
Fx=c1*lambda*fs/(1-lambda);                    %  Actual braking force
Fx_hat=c1_hat*lambda*fs_hat/(1-lambda);    %  Nominal braking force
%=============================================================
%Outputs
y(1)=Fx;
y(2)=Fx_hat;
%=============================================================
```

(c) RBFNN-Prediction Based Controller Subsystem

(c1) NNprediction1 function

```
function y = NNprediction1(x)
global  cc bb  NL gamma
e=x(1);
de=x(2);
xi=[e;de];
h=zeros(NL,1);
for j=1:1:NL
   h(j)=exp(-norm(xi-cc(:,j))^2/(2*bb(j)*bb(j)));
end
for i=1:1:NL
   W(i)=1/gamma*e*h(i);
end
for i=1:1:NL
  y(i)=W(i);
end
```

(c2) NNprediction2 function

```
function y = NNprediction2(x)
global  R  It_hat  cc  bb NL  hh  mt_hat  mt  It  lambda_opt
e=x(1);
de=x(2);
lambda=x(4);
vx=x(5);
t=x(7);
Fx=x(8);
Fx_hat=x(9);
dlambda_d=20* lambda_opt *exp(-20*t);      % Derivative of the desired value of wheel slip
W1=x(10);W2=x(11);W3=x(12);W4=x(13);W5=x(14);
W=[W1 W2 W3 W4 W5 ]';
xi=[e;de];
h=zeros(NL,1);
for j=1:1:NL
   h(j)=exp(-norm(xi-cc(:,j))^2/(2*bb(j)*bb(j)));
end
L_hat=W'*h;                                % Approximation of lumped uncertainty L
f=-(Fx*(1-lambda)/mt+R^2*Fx/It)/vx;
f_hat=-(Fx_hat*(1-lambda)/mt_hat+R^2*Fx_hat/It_hat)/vx;
g=R/(vx*It);
g_hat=R/(vx*It_hat);
Tb=(-1/(g_hat*hh))*(e+hh*(f_hat+L_hat- dlambda_d));
L=(f-f_hat)+(g-g_hat)*Tb;                  % Lumped uncertainty
y(1)=Tb;
y(2)=L_hat;
y(3)=L;
%=============================================================
```

(e) Quarter_Vehicle_Model function

```
function y= Quarter_Vehicle_Model (x)
global  R  mt  It
lambda=x(4);
vx=x(5);
Fx=x(8);
Tb=x(10);
vx_dot=-Fx/mt;
lambda_dot=-(Fx*(1-lambda)/mt+R^2*Fx/It)/vx+(R*Tb)/(vx*It);
y(1)=vx_dot;
y(2)=lambda_dot;
%=============================================================
```

References

[1] J.Y. Wong, Theory of Ground Vehicles, third ed., Wiley, New York, 2001.
[2] J. Lee, J. Choi, K. Yi, Lane-keeping assistance control algorithm using differential braking to prevent unintendedlane departures, Control Eng. Pract. 23 (2014) 1–13.
[3] D. Aleksendric, D.C. Barton, Neural network prediction of disk brake performance, Tribol. Int. 42 (7) (2009) 1074–1080.
[4] V. Ćirović, D. Aleksendrić, Adaptive neuro-fuzzy wheel slip control, Expert Syst. Appl. 40 (13) (2013) 5197–5209.
[5] T.A. Johansen, I. Petersen, J. Kalkkuhl, J. Ludemann, Gain scheduled wheel slip control in automotive brake systems, IEEE Trans. Control Syst. Technol. 11 (6) (2003) 799–811.
[6] Y. Qiu, X. Liang, Z. Dai, Backstepping dynamic surface control for an anti-skid braking system, Control Eng. Pract. 42 (2015) 140–152.
[7] E. Dincmen, B.A. Guvenc, T. Acarman, Extremum-seeking control of abs braking in road vehicles with lateral force improvement, IEEE Trans. Control Syst. Technol. 22 (1) (2014) 230–237.
[8] S. Kar, S. Das, P.K. Ghosh, Applications of neuro fuzzy systems: a brief review and future outline, Appl. Soft Comput. 15 (2014) 243–259.
[9] R. de Castro, R.E. Araujo, D. Freitas, Wheel slip control of EVs based on sliding mode technique with conditional integrators, IEEE Trans. Ind. Electron. 60 (8) (2013) 3256–3271.
[10] A. Pisano, M. Tanelli, A. Ferrara, Switched/time-based adaptation for second-order sliding mode control, Automatica 64 (2016) 126–132.
[11] A.L. Masich, H.V. Blavi, J.M.B. Moncusí, J.M. Altés, L.M. Salamero, Sliding-mode-control-based boost converter for high- voltage-low-power applications, IEEE Trans. Ind. Electron. 62 (1) (2015) 229–237.
[12] S. Biricik, H. Komurcugil, Optimized sliding mode control to maximize existence region for single-phase dynamic voltage restorers, IEEE Trans. Ind. Inf. 12 (4) (2016) 1486–1497.
[13] R.E. Precup, M.B. Radac, R.C. Roman, E.M. Petriu, Model-free sliding mode control of nonlinear systems: algorithms and experiments, Inf. Sci. 381 (2017) 176–192.
[14] C.F. Hsu, Intelligent exponential sliding-mode control with uncertainty estimator for antilock braking systems, Neural Comput. Appl. 27 (6) (2016) 1463–1475.
[15] Y. Tang, Y. Wang, M. Han, Q. Lian, Adaptive fuzzy fractional-order sliding mode controller design for antilock braking systems, J. Dyn. Syst. Meas. Control 138 (4) (2016) p041008.
[16] A.B. Sharkawy, Genetic fuzzy self-tuning PID controllers for antilock braking systems, Eng. Appl. Artif. Intell. 23 (7) (2010) 1041–1052.
[17] D. Aleksendrić, Z. Jakovljević, J. Park, I.W. Sandberg, Intelligent control of braking process, Expert Syst. Appl. 39 (14) (2012) 11758–11765.
[18] S. Park, J.P. Hwang, E. Kim, H. Lee, H.G. Jung, A neural network approach to target classification for active safety system using microwave radar, Expert Syst. Appl. 37 (3, 15) (2010) 2340–2346.
[19] X. Peng, H. Zhe, G. Guifang, X. Gang, C. Binggang, L. Zengliang, Driving and control of torque for direct-wheel-driven electric vehicle with motors in serial, Expert Syst. Appl. 38 (1) (2011) 80–86.
[20] S. Kanarachos, A.M. Dizqah, G. Chrysakis, M.E. Fitzpatrick, Optimal design of a quadratic parameter varying vehicle suspension system using contrast-based Fruit Fly Optimisation, Appl. Soft Comput. 62 (2018) 463–477.
[21] R.E. Precup, M.C. Sabau, E.M. Petriu, Nature-inspired optimal tuning of input membership functions of Takagi-Sugeno-Kang fuzzy models for Anti-lock Braking Systems, Appl. Soft Comut. 27 (2015) 575–589.
[22] C.F. Hsu, C.M. Lin, Y.R. Guan, Supervisory adaptive dynamic RBF-based neural-fuzzy control system design for unknown nonlinear systems, Appl. Soft Comput. 13 (4) (2013) 1620–1626.
[23] C.K. Lin, Radial basis function neural network-based adaptive critic control of induction motors, Appl. Soft Comput. 12 (6) (2011) 1640–1649.
[24] Y.Y. Fu, C.J. Wu, C.N. Ko, Radial basis function networks with hybrid learning for system identification with outliers, Appl. Soft Comput. 11 (3) (2011) 2278–2283.
[25] C.F. Hsu, Adaptive dynamic RBF neural controller design for a class of nonlinear systems, Appl. Soft Comput. 11 (8) (2011) 4607–4613.
[26] S.N. Qasem, S.M. Shamsuddin, Radial basis function network based on time variant multi-objective particle swarm optimization for medical diseases diagnosis, Appl. Soft Comput. 11 (1) (2011) 1427–1438.
[27] J. Park, I.W. Sandberg, Universal approximation using radial-basis-function networks, Neural Comput. 3 (2) (1991) 246–257.
[28] H. Yu, T. Xie, S. Paszczynski, B.M. Wilamowski, Advantages of radial basis function networks for dynamic system design, IEEE Trans. Ind. Electron. 58 (12) (2011) 5438–5450.
[29] X. Zhu, N. Wang, Cuckoo search algorithm with membrane communication mechanism for modeling overhead crane systems using RBF neural networks, Appl. Soft Comput. 56 (2017) 458–471.
[30] M. Robnik-Šikonja, Data generators for learning systems based on RBF networks, IEEE Trans. Neural Networks Learn. Syst. 27 (5) (2016) 926–938.
[31] J. Tian, M. Li, F. Chen, N. Feng, Learning subspace-based RBFNN using coevolutionary algorithm for complex classification tasks, IEEE Trans. Neural Networks Learn. Syst. 27 (1) (2016) 47–61.
[32] A. Alexandridis, E. Chondrodima, H. Sarimveis, Cooperative learning for radial basis function networks using particle swarm optimization, Appl. Soft Comput. 49 (2016) 485–497.
[33] J. Wu, J. Long, M. Liu, Evolving RBF neural networks for rainfall prediction using hybrid particle swarm optimization and genetic algorithm, Neurocomputing 148 (2015) 136–142.
[34] H. Mirzaeinejad, M. Mirzaei, A novel method for non-linear control of wheel slip in anti-lock braking systems, Control Eng. Pract. 18 (8) (2010) 918–926.
[35] M. Jafari, M. Mirzaei, H. Mirzaeinejad, Optimal nonlinear control of vehicle braking torques to generate practical stabilizing yaw moments, Int. J. Automot. Mech. Eng. 11 (2015) 2639–2653.
[36] M. Mirzaei, H. Mirzaeinejad, Fuzzy scheduled optimal control of integrated vehicle braking and steering systems, IEEE/ASME Trans. Mechatron. 22 (2017) 2369–2379.
[37] H. Mirzaeinejad, M. Mirzaei, Optimization of nonlinear control strategy for anti-lock braking system with improvement of vehicle directional stability on split-μ roads, Transp. Res. Part C: Emerg. Technol. 46 (2014) 1–15.
[38] H. Mirzaeinejad, M. Mirzaei, R. Kazemi, Enhancement of vehicle braking performance on split-μ roads using optimal integrated control of steering and braking systems, Proc. Inst. Mech. Eng. Part K: J. Multi-Body Dyn. 230 (4) (2015) 401–415.
[39] A.E. Bryson, Y.C. Ho, Applied Optimal Control, Hemisphere, Washington DC, 1975.
[40] E.J. Park, D. Stoikov, L.F.D. Luz, A. Suleman, A performance evaluation of an automotive magnetorheological brake design with a sliding mode controller, Mechatronics 16 (7) (2006) 405–416.
[41] D.E. Smith, J.M. Starkey, Effects of model complexity on the performance of automated vehicle steering controllers: model development, validation and comparison, Veh. Syst. Dyn. 24 (1995) 163–181.
[42] W.H. Chen, D.J. Balance, P.J. Gawthrop, Optimal control of nonlinear systems: a predictive control approach, Automatica 39 (4) (2003) 633–641.
[43] J.J.E. Slotine, W. Li, Applied Nonlinear Control, Prentice Hall, Englewood Cliffs, 1991.
[44] J. Nocedal, S.J. Wright, Numerical Optimization: Springer Series in Operation Research and Financial Engineering, 2006.
[45] D.S. Broomhead, D. Lowe, Multivariable functional interpolation and adaptive networks, Complex Syst. 2 (1988) 321–355.
[46] T. Chen, H. Chen, Approximation capability to functions of several variables, nonlinear functionals, and operators by radial basis function neural networks, IEEE Trans. Neural Netw. 6 (1995) 904–910.
[47] K.R. Buckholtz, Reference Input Wheel Slip Tracking Using Sliding Mode Control, SAE Technical Paper 2002-01-0301, 2002.
[48] S. Zheng, H. Tang, Z. Han, Y. Zhang, Controller design for vehicle stability enhancement, Control Eng. Pract. 14 (12) (2006) 1413–1421.